

PAPER • OPEN ACCESS

## Quantum size effect in single-crystalline bismuth nanorods

To cite this article: E A Sedov *et al* 2017 *J. Phys.: Conf. Ser.* **929** 012088

View the [article online](#) for updates and enhancements.

### Related content

- [Size-dependent thermoelectricity in nanowires](#)  
Shadyar Farhangfar
- [First-Principles Calculations of the Quantum Size Effects on the Stability and Reactivity of Ultrathin Ru\(0001\) Films](#)  
Wu Ming-Yi, Jia Yu and Sun Qiang
- [Quantum Size Effect in Thin Bismuth Films](#)  
Hajime Asahi, Takabumi Humoto and Akira Kawazu

# Quantum size effect in single-crystalline bismuth nanorods

E A Sedov<sup>1</sup>, K –P Riikonen<sup>2</sup> and K Yu Arutyunov<sup>1,3</sup>

<sup>1</sup> National Research University Higher School of Economics, Moscow, 101000, Russia

<sup>2</sup> Nano Science Center, Department of Physics, University of Jyväskylä, PB 35, 40014, Jyväskylä, Finland

<sup>3</sup> P.L. Kapitza Institute for Physical Problems RAS, 119334, Moscow, Russia

E-mail: Sedov1993@yandex.ru

**Abstract.** In a metal sample, where at least one of the dimensions is comparable with the de Broglie wavelength of conduction electrons, the quantum size effects (QSE) should be observed. QSEs manifest themselves as non-monotonic dependencies of various material properties as function of relevant dimension. QSE should be particularly noticeable in materials with charge carrier(s) effective mass less than the free electron mass. Bismuth is one of the most suitable semi-metal to observe QSE due to small effective masses and small the Fermi energy. However, bismuth has a high anisotropic energy spectrum. Hence to observe QSE which can be interpreted with reasonable accuracy, it is mandatory to fabricate single-crystal nanostructure with known orientation of crystallographic axes. In this paper several short bismuth nanowires (nanorods) were investigated, and oscillating dependence of electric resistance on effective cross section was found. Theoretical calculations provide a reasonable agreement with experiment. The quantum-size phenomena are important for operation of a wide spectrum of nanoelectronic devices.

## 1. Introduction

The laws of classical physics might describe well the behaviour of macroscopic objects, but if dimension(s) are reduced down to certain scales, one might observe qualitatively different quantum phenomena. The origin of the QSE is related to the text-book problem of energy level quantization of a particle with mass  $m$  confined inside a potential well with characteristic dimension  $a$ :  $E(n) = n^2 \hbar^2 \pi^2 / 2ma^2$ ,  $n = 1, 2, 3 \dots$ . QSEs affect various electronic properties of metals: electric conductivity, Hall and thermoelectric coefficients, reflectivity, etc. [1]. However in a typical metal with effective masses  $m^*$  comparable to free electron mass  $m_0$  QSEs manifest at scales of about 1 nm. While in materials with  $m^* \ll m$ , like antimony, bismuth or their alloys [2], the QSEs can be observed at scales  $\sim 100$  nm achievable by modern nanofabrication.

In bismuth there are two types of charges: 'heavy' T-holes with  $m^h \approx m_0$  and 'light' L-electrons with  $m^e \ll m_0$  (Fig. 1a). Heavy T-holes fix the energy of the Fermi level and, as a first approximation, one might neglect the energy quantization effect for T-holes. While for L-electrons one might expect the manifestation of QSE (Fig. 1b). As the energy spectrum of bismuth is strongly anisotropic, the



expected phenomena should dependent on particular orientation of the sample with respect to its crystallographic axes.

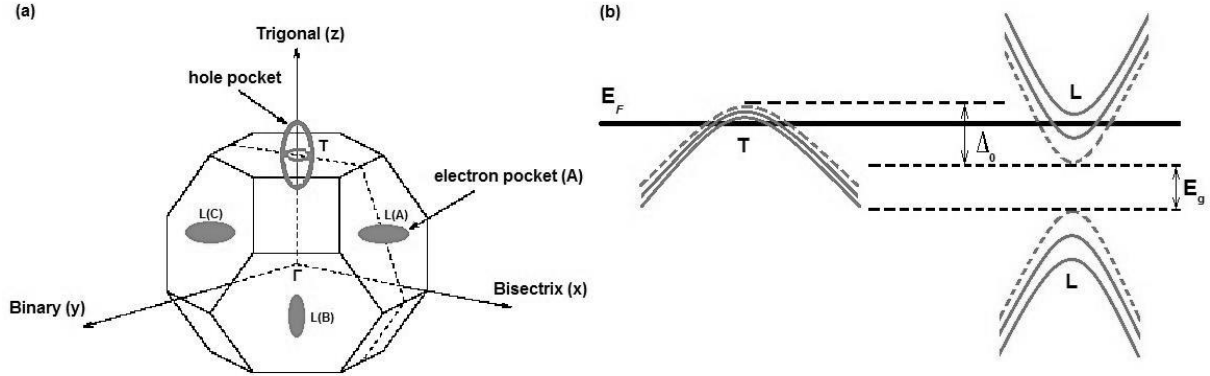


Fig. 1. (a) Brillouin zone and Fermi surface of bulk bismuth with three ‘light’ L-electron and one ‘heavy’ T-hole pockets. (b) Energy spectrum of bismuth. Dashed lines stand for bulk, while solid lines correspond to splitting of energy levels due to QSE.

First observations of QSE refer to early 1960-th including both experimental [3] and theory [4] studies. Later, other low-dimensional structures were investigated: microcylinders [5], nanowires [6, 7] and point contacts [8, 9]. Unfortunately, experiments with bundles of nanowires [6, 7] can provide only qualitative results because the contributions of individual nanowires are averaged. The experiments realized with scanning tunneling microscope (STM) technique [8, 9] demonstrated clear size-dependent change of electrical conductivity. However, the results of STM experiments [8, 9] are difficult to interpret, because the crystallographic orientation and the shape of an STM-pulled point contacts are not clearly defined.

In this work we experimentally demonstrate that electric resistivity of single-crystalline bismuth nanorods non-monotonically varies with reduction of cross section. The size dependence of resistance oscillates and can be interpreted in terms of relevant theoretical model [10].

## 2. Theory

The model [10] assumes parabolic  $E(\mathbf{k})$  dependence for bismuth spectrum [11, 12] both for T-holes and L-electrons with the corresponding effective mass diagonal elements (in units of free-electron mass) for holes  $m_x^h=m_y^h=0.059$ ,  $m_z^h=0.634$  and electrons  $m_x^e=0.00139$ ,  $m_y^e=0.291$ ,  $m_z^e=0.0071$  (Fig. 1a). The energy gap is  $E_g = 13.7 \pm 0.1 \text{ meV}$  in L-point and the band overlap energy is  $\Delta = 38 \text{ meV}$  (Fig. 1b).

Model [10] solves Boltzmann kinetic equation for bismuth nanowire of rectangular cross section  $w*t$ , where  $w$  is width and  $t$  is thickness. Following Ref. 10 one obtains the oscillatory dependence of electrical resistivity vs. cross section:

$$R^e = \left( \frac{2 q_e^2}{\pi \hbar} \frac{1}{\varrho} \frac{\mu_x^e}{m_z^e} \sum_{m,n=1}^{\lfloor r_w \rfloor, \lfloor r_t \rfloor} \frac{(2\hbar/V_0)^2 \sqrt{U_{mn}^e}}{\sum_{m',n'=1}^{\lfloor r_w \rfloor, \lfloor r_t \rfloor} \Lambda_{m'n'}^{mn} / \sqrt{U_{m'n'}^e}} \right)^{-1} \quad (1)$$

where  $U_{mn}^e \equiv 1 - (m/r_w)^2 + (\mu_y^e/\mu_x^e)[1 - (n/r_t)^2]$ ;  $\Lambda_{m'n'}^{mn} \equiv (2 + \delta_{mm'})(2 + \delta_{nn'})$ , here  $\delta_{ab}$  is Kronecker delta function;  $\varrho \equiv N/\Omega$  is the value of the carriers density. Parameters  $r_w \equiv w/w_0$  and  $r_t \equiv t/t_0$  are width and thickness of nanowire, normalized by the relevant dimensions  $w_0 = \hbar\pi/(2M_x\Delta_x)^{1/2}$  and  $t_0 = \hbar\pi/(2M_y\Delta_y)^{1/2}$  corresponding to metal-to-insulator transition: when the gap opens between the lowest L-electron and the highest T-hole bands (Fig. 1b). Here  $M_{x,y} \equiv (m_{x,y}^e m_{x,y}^h)/(m_{x,y}^e + m_{x,y}^h)$  and  $\mu_{x,y}^e \equiv (\Delta_{x,y} m_{x,y}^h)/(m_{x,y}^e + m_{x,y}^h)^{-1}$ ,  $\Delta_{x,y}$  is the energy bands overlap due to confinement of charge carriers in corresponding direction x or y. The outer summation

accounts for contribution of the different  $(m, n)$  sub-bands. Formally, to calculate the total electric conductivity one should also consider the T-hole contribution. However, as for certain particular directions (e.g. along the bisectrix axis) the T-hole masses are significantly larger than for L-electrons, one can neglect the QSE for holes. The observation simplifies the calculation allowing one to consider the hole contribution to integral electric resistivity as an additive size-independent term.

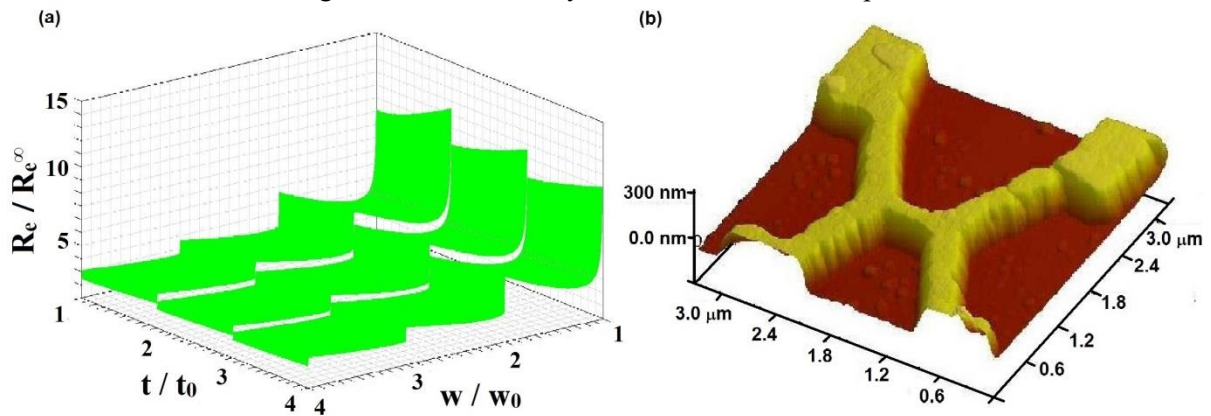


Fig. 2. (a) Calculated electron resistivity  $R_e$ , normalized by the bulk value  $R_e^\infty$ , for bismuth nanowire of rectangular cross section  $w*t$  cut along bisectrix axis as function of thickness  $t$  and width  $w$  in units of threshold values  $t_0$  and  $w_0$ , corresponding to metal-to-insulator transition. (b) AFM image of typical bismuth nanostructure on mica substrate after several sessions of ion milling.

Obviously for material with highly anisotropic energy spectrum as bismuth, the electric resistivity  $R_e(w, t)$  depends on orientation of the sample relative to crystallographic axes. If the sample is cut along high-symmetry crystallographic axis, Eq. (1) provides rather simple  $R_e(w, t)$  dependence (Fig. 2a). If one cuts the sample along an arbitrary direction, the QSE in all three non-equivalent L-pockets of the Fermi surface will result in a complicated  $R_e(w, t)$  dependence with secondary maxima and minima. It should be noted that a particular experimentally observed  $R_e(\text{cross section})$  dependence is affected not only by the effective diameter  $(w*t)^{1/2}$ , but also by the actual values of width  $w$  and thickness  $t$ , representing a 'slice' of three-dimensional  $R_e(w, t)$  function (Fig. 2a).

### 3. Experimental

In order for detect the quantum size effect we fabricated several single crystal bismuth nanorods with typical dimensions: length 0.8-1  $\mu\text{m}$ , width 0.3-0.4  $\mu\text{m}$  and thickness 0.2-0.3  $\mu\text{m}$ . All nanostructures were designed for measuring resistance in four probe configuration (Fig. 2b).

For QSE studies several approaches have been proposed [5, 7, 13, 14]. In this paper we used a standard lift-off e-beam lithography on high speed ( $\sim 1$  nm/s at  $10^{-6}$  mbar) pure bismuth deposited film on mica substrate heated to 140  $^\circ\text{C}$ . Atomic force (AFM) and scanning electron (SEM) microscope analyses revealed polycrystalline structure of the films with the grain size up to 1.5  $\mu\text{m}$ . X-ray analysis of co-deposited wide films showed that the trigonal axis in each grain is perpendicular to the substrate plane. Contrary to Ref. [14], where long bismuth nanowires containing multiple grains connected in series, our lithographically fabricated structures (the 'nanorods') were made deliberately rather short to enable the very central part of the sample (the 'body') be a single crystal (Fig. 2b).

To observe the QSE in between the sessions of resistivity measurements we used low-energy  $\text{Ar}^+$  directional ion milling to reduce the effective diameter of the nanorods [15]. The method permits progressive removal of material from the surface just by few atomic layers. At the utilized acceleration energies  $< 1$  keV the penetration depth of  $\text{Ar}^+$  ions inside the metal matrix is minimal  $< 2$  nm being comparable to the thickness of chemically corrupted layer at the very surface [16]. The technique enables the consistent reduction of a nanostructure cross section  $(w*t)^{1/2}$  down to the sub-50 nm scales

[17]. AFM analysis was used to evaluate the dimensions of the structures after each session of ion milling [16].

#### 4. Results and discussion

Between sessions of ion beam milling we measured the resistance  $R$  of bismuth nanorods as function of their transverse dimensions: width  $w$  and thickness  $t$ . We examined several samples and all of them demonstrated non-monotonic  $R_e(w,t)$  dependencies (Fig. 3). In the thinnest structures approaching  $(w*t)^{1/2} \sim 50$  nm we have observed a pronounced increase of electric resistance, which can be associated with QSE-mediated metal-to-semiconductor transition [17]. However, even the wider samples at scales  $(w*t)^{1/2} < 200$  nm demonstrate peaks of electric resistivity (= dips of conductivity), corresponding to crossing of the size-quantized energy bands and the Fermi level (Fig. 1b).

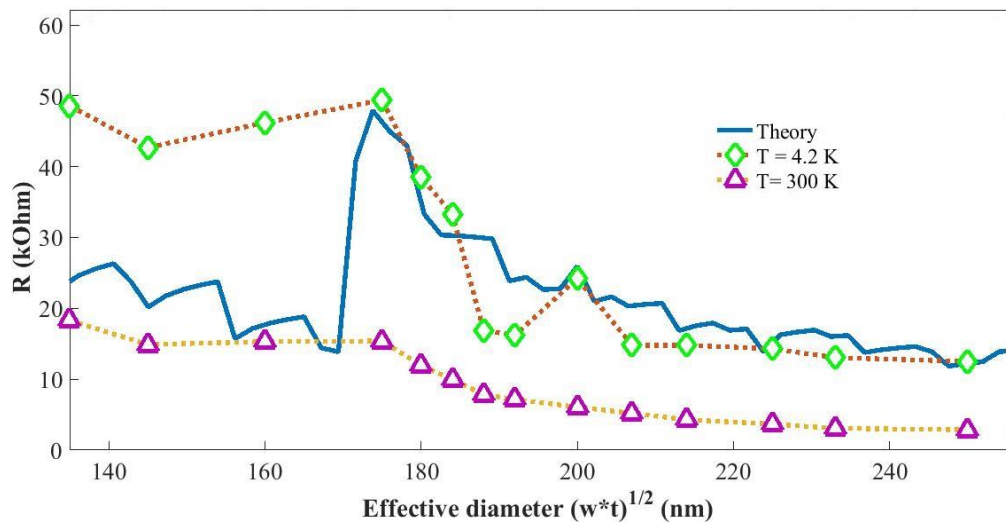


Fig. 3.  $R(w,t)$  dependence for bismuth nanowire. Triangles correspond to room temperature and squares stand for  $T=4.2$  K data. Dashed lines, connecting experimental points, are guides for eye. Solid line is the best theory fit using Eq. (1).

In Fig. 3 one can trace a certain correlation between the calculation based on model [10] and experiment, but the agreement is far from being perfect. Presumably the mismatch originates from uncertainty in orientation of the sample axis (= current lines) against the crystallographic axes of the central grain, forming the 'body' of the sample. Though for electric measurements we have used 4-probe configuration, the relatively short length of the nanorod compared to width and thickness, does not allow to consider the measuring probes as non-invasive and, hence, the current lines are not strictly parallel to each other. The best-fit theory dependence in Fig. 3 considers the simplified arrangement: the bisectrix axis in the central grain ('body') is parallel to the current lines. Then the two main peaks originate from L-electrons with minimal effective mass  $m_x^e \approx 0.00139m_0$ . Small peaks are contributions from two other L-electron pockets with larger effective masses. Heavy T-holes contribute to electric conductivity with much less pronounced size dependence due to their large effective mass  $m^h \gg m^e$ . Formally better agreement between experiment and theory can be achieved if to consider the contributions of several single crystalline grains with mismatched binary and orientations (e.g. the central grain and the two neighbors from the probes) connected in series. However as the X-ray structural analyses of each particular nanostructure could not be performed (we do not have such facilities) the 'improvement' would be speculative. One should also notice that reduction of temperature down to  $T=4.2$  K makes the experimental  $R_e(w,t)$  dependencies more 'sharp'. The observation reflects the obvious fact that finite temperature  $T$  broadens each size-quantized energy level by  $k_B T$  making the crossing with Fermi level 'washed out'.

## 5. Conclusions

We fabricated short bismuth's single-crystalline nanorods and measured their resistivity as function of effective cross section  $(w*t)^{1/2}$ . The  $R(w,t)$  data demonstrated clear non-monotonic dependence, which is consistent with model [10] that takes into account the quantum size effects in bismuth nanowires with rectangular cross section. The agreement between experiment and theory is not perfect, presumably, due to difficulty to fabricate a truly single-crystalline one-dimensional nanostructure with well defined orientation against crystallographic axes. Nevertheless our observations can be considered to be in a semi-quantitative (or at least - qualitative) agreement with theory predictions.

The results suggest that production of the next generation of ultra-small nanoelectronic devices should take into account the quantum size effects, as it is a universal phenomena and should affect basically all electronic properties of such tiny objects [1].

## Acknowledgements

The article was prepared within the framework of the Academic Fund Program at the National Research University Higher School of Economics (HSE) in 2016 (grant No. 16-05-0029) and supported within the framework of a subsidy granted to the HSE by the Government of the Russian Federation for the implementation of the Global Competitiveness Program.

## References

- [1] Tringides M C, Jatochowski M and Bauer E 2007 *Phys. Today* **60** 50-54
- [2] Lutski V N, 1970 *Phys. Stat. Sol.* **1** 199-220
- [3] Ogrin Yu V, Lutskii V N and Elinson M I 1966 *Zh. Exper. Teor. Fiz. Pisma.* **3** 114-118
- [4] Sandomirskii V 1967 *BSov. Phys. JETP* **25** 101-106
- [5] Nikolaeva A, Huber T, Konopko L, Tsurkan A 2010 *J. Low. Temp. Phys.* **158** 530-535
- [6] Sun X, Zhang Z and Dresselhaus M S 1999 *Appl. Phys. Lett.* **74** 4005-4007
- [7] Heremans J et. al 2000 *Phys. Rev. B* **61** 2921-2930
- [8] Costa-Krämer J L Garcia N and Olin H 1997 *Phys. Rev. Lett.* **78** 4990-4993
- [9] Rodrigo J G Garcia-Martín A Sáenz J J and Vieira S 2002 *Phys. Rev. Lett.* **88** 246801-1 - 246801-4
- [10] Farhangfar S 2006 *Phys. Rev. B* **74** 205318-1 -205318-5
- [11] Lax B and Mavroides J G 1960 *Solid State Physics* (Academic Press, New York)
- [12] Zhang Z et. al 2000 *Phys. Rev. B* **61** 4850-4861
- [13] Arutyunov K Yu Ryyanen T V Pekola J P and Pavolotski A B 2001 *Phys. Rev. B* **63** 092506-1 - 092506-4
- [14] Farhangfar S 2007 *Phys. Rev. B* **76** 205437-1 - 205437-4
- [15] Savolainen M et. al 2004 *Appl. Phys. A* **79** 1769 -1773
- [16] Zgirski M et. al 2008 *Nanotechnology* **19** 055301-1 -055301-6
- [17] Sedov E A Riikonen K-P and Arutyunov K Yu 2017 *to be published elsewhere*